

Pursuing Feature Separation based on Neural Collapse for Out-of-Distribution Detection

Yingwen Wu*
Ruiji Yu
Xinwen Cheng
Zhengbao He
Xiaolin Huang

May 29, 2024

Abstract

In the open world, detecting out-of-distribution (OOD) data, whose labels are disjoint with those of in-distribution (ID) samples, is important for reliable deep neural networks (DNNs). To achieve better detection performance, one type of approach proposes to fine-tune the model with auxiliary OOD datasets to amplify the difference between ID and OOD data through a separation loss defined on model outputs. However, none of these studies consider enlarging the feature disparity, which should be more effective compared to outputs. The main difficulty lies in the diversity of OOD samples, which makes it hard to describe their feature distribution, let alone design losses to separate them from ID features. In this paper, we neatly fence off the problem based on an aggregation property of ID features named Neural Collapse (NC). NC means that the penultimate features of ID samples within a class are nearly identical to the last layer weight of the corresponding class. Based on this property, we propose a simple but effective loss called OrthLoss, which binds the features of OOD data in a subspace orthogonal to the principal subspace of ID features formed by NC. In this way, the features of ID and OOD samples are separated by different dimensions. By optimizing the feature separation loss rather than purely enlarging output differences, our detection achieves SOTA performance on CIFAR benchmarks without any additional data augmentation or sampling, demonstrating the importance of feature separation in OOD detection. The code will be published.

*Y. Wu, R. Yu, X. Cheng, Z. He and X. Huang are with the Department of Automation, Shanghai Jiao Tong University, 200240 Shanghai, P.R. China. Email: yingwen_wu@sjtu.edu.cn

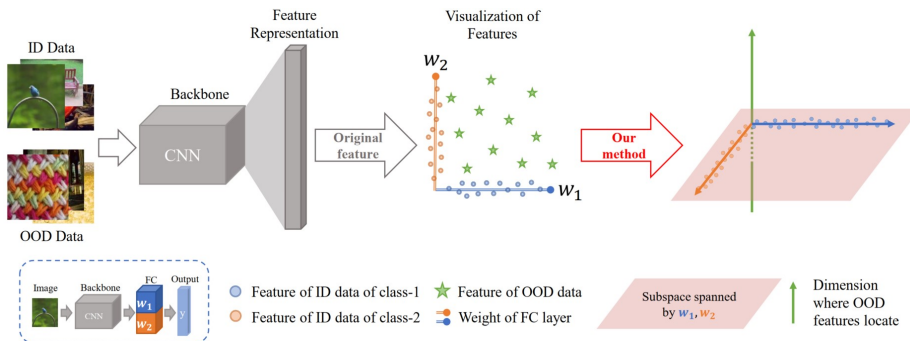


Figure 1: Overview of our method. An example of a well-trained binary classification network, where w_i denotes the i -th weight of the last fully connected layer. The features of ID samples within a class are nearly identical to the weight of the corresponding class, which is known as Neural Collapse. Based on this property, we propose to constrain OOD features to lie in dimensions orthogonal to the FC weight subspace to explicitly separate the feature manifold between ID and OOD data.

1 Introduction

In the open world, deep neural networks (DNNs) encounter a diverse range of input images, including in-distribution (ID) data that shares the same distribution as the training data, and out-of-distribution (OOD) data, which has labels that are disjoint from those of the ID cases. Facing the complex input environment, a reliable network system must not only provide accurate predictions for ID data but also recognize unseen OOD data. This necessity gives rise to the critical problem of OOD detection [3, 31], which has garnered significant attention in recent years, particularly in safety-critical applications.

A rich line of studies detect OOD samples by exploring the differences between ID and OOD data in terms of model outputs [13, 33], features [43, 57, 44], or gradients [15, 50]. However, it has been observed that models trained solely on ID data can make over-confident predictions on OOD data, and the features of OOD data can intermingle with those of ID features [13, 44]. To develop more effective detection algorithms, a category of works focus on the utilization of auxiliary OOD datasets, which can significantly improve detection performance on unseen OOD data. One classical method, called Outlier Exposure (OE, [14]), employs a cross-entropy loss between the outputs of OOD data and uniformly distributed labels to fine-tune the model. Additionally, Energy [33] proposes using the energy function as its training loss and designs an energy gap between ID and OOD data. Building on these proposed losses, recent works have concentrated on improving the quality of auxiliary OOD datasets through data augmentation [48, 49, 55] or data sampling [35, 5, 19] algorithms to achieve better detection performance.

Existing losses designed for auxiliary OOD data primarily focus on increasing

the output discrepancy between ID and OOD samples [14, 33]. However, **NONE** of these approaches consider enhancing the separability in the feature space. Insights from knowledge distillation [11] and contrastive learning [26] have demonstrated that optimizing compactness or dispersion in the feature space is equally or even more important than enforcing similar constraints in the output space. Furthermore, previous detection score function design has shown the importance of employing feature information [43, 44, 57], which can greatly improve detection performance. Therefore, when tackling the fine-tuning problem using auxiliary OOD data, we propose that it is crucial to **separate the features between ID and OOD data**, rather than merely enlarging their output differences.

Designing an effective feature separation loss for ID and OOD data is inherently challenging due to the diversity of OOD samples, which belong to various categories. This diversity results in a dispersion of their features and difficulty in describing their feature distribution. Consequently, common feature separation losses, such as maximizing the distance between the average features of different classes [36] or increasing the Kullback-Leibler divergence between ID and OOD feature distributions [25], are not suitable in our cases. Despite the intricate distribution of OOD features posing a significant obstacle, in this paper, we derive solutions from the properties of ID features.

A recent observation named Neural Collapse [40] gives us an inspiration, which reveals that the penultimate features of ID samples within a class are nearly identical to the last fully connected (FC) layer’s weights of the corresponding class. Conversely, the features of OOD samples are scattered haphazardly throughout the feature space. A direct illustration ¹ can be seen in Figure 1. Leveraging the property of ID features, we propose to constrain the features of OOD data on dimensions orthogonal to the subspace (denoted as \mathbf{W}) spanned by FC weights. The dimension of \mathbf{W} equals to the number of ID categories, while the overall feature space dimension is significantly larger. Consequently, there are numerous redundant dimensions available for OOD features, indicating the feasibility of our method. To pursue this orthogonality, we introduce a loss function named OrthLoss (*ref.* Eq3), which calculates the cosine similarity between OOD features and the weights of the final FC layer. By optimizing this simple yet effective loss to zero, we ensure that OOD features are distributed in entirely different dimensions from ID features, thereby enhancing their separability. Our approach utilizes the NC property of ID features, allowing us to avoid modeling OOD feature distributions while effectively segregating ID and OOD features. The overall method can be widely applied as a stronger baseline compared to OE [14], and seamlessly integrated with other approaches like ATOM[5], POEM[35], etc[48, 49] by replacing the OE loss with our OrthLoss.

We conduct extensive experiments over representative OOD detection setups, achieving the SOTA performance without any data augmentation or sampling algorithms [35, 49] on CIFAR10 and CIFAR100 benchmarks. For example, on

¹For binary classification, NC indicates that the angle between w_1 and w_2 should be 180° . But in order to show the general case of higher dimensions, we depict an angle of 90° in the figure.

the CIFAR100 benchmark, by using our feature separation loss, we achieve the average FPR95 of 29.58% and AUROC of 94.01%, outperforming the traditional OE [14] method by 8.19% on FPR95. Furthermore, our method exhibits a very stable performance while comparable methods like DAL [48] struggle with a high fluctuation, as Sec 4.4 shows. The contribution of our paper is summarized as follows:

- We are the first to propose the concept of feature separation when using auxiliary OOD data to fine-tune models, while previous works pay more attention to the output separation, providing new insights into the design of OOD data loss functions.
- To overcome the difficulty caused by OOD data diversity, we propose a feature separation loss based on the neural collapse property of ID features, which constrains OOD features to lie in dimensions where ID features are scarcely distributed.
- Our SOTA detection performance on representative OOD detection settings verify the effectiveness of our feature separation loss, implying that our loss can be a stronger baseline for future researches.

2 Related work

Post-hoc Detection. Given a model that is only trained by ID data, post-hoc detection approaches design score functions based on it to distinguish ID and OOD data. One type method named density-based [28, 22, 58, 21, 18, 6] is to explicitly model the ID data with some probabilistic models and flag test data in low-density regions as OOD samples. More popular approaches are to derive confidence score based on model outputs [13, 30, 33], features [43, 57, 44, 28, 37, 8, 37, 8, 47] or gradients [15, 50, 27, 34, 42, 17]. For example, the classical maximum softmax probability method [13] utilizes the model output probability of the predicted class as a confidence score and then identifies samples with low scores as OOD data.

Contrastive Learning based Detection. Different from post-hoc methods based on vanilla-trained models, such methods generally apply contrastive losses defined on ID data in the model training process to obtain better feature representations for OOD detection. For example, KNN+ [44] utilizes the SupCon loss [20], which encourages alignment of features within a class and dispersion of features of different classes, to train a network to obtain greater differentiation between ID and OOD samples. Besides, CSI[45] contrasts original samples with their distributionally-shifted augmentations to improve detection performance. Recent advancements, such as CIDER [36], combine a compactness loss to cluster samples near their class prototypes and a dispersion loss to maximize angular distances between different class prototypes, providing a more direct and clearer geometric interpretation for the disparity between ID and OOD samples.

Auxiliary OOD Data based Detection. With access to part of OOD data, previous works design training algorithms to utilize auxiliary OOD data

for OOD detection. One type method is to propose unsupervised training loss functions [14, 33, 2], such as the Kullback-Leibler divergence between OOD output probability and uniformly distributed label [14], to fine-tune the model. Based on the proposed losses, another type is to select OOD data close to the decision boundary [35] or conduct data augmentation through adversarial attack [5, 48] and model perturbations [49] in the training process, which can tight the boundary so that pushing unseen OOD data far away from it. In general, using auxiliary OOD data in the training process can significantly improve detection performance, achieving better results compared with other detection approaches.

3 Method

3.1 Preliminary

OOD Detection Problem. The framework for OOD detection is outlined as follows. We consider a classification problem involving C classes, where \mathcal{X} represents the input space and \mathcal{Y} denotes the label space. The joint data distribution over $\mathcal{X} \times \mathcal{Y}$ is referred to as $D_{\mathcal{X}\mathcal{Y}}$. Let $f_\theta : \mathcal{X} \mapsto \mathcal{Y}$ be a model trained on samples drawn independently and identically distributed (*i.i.d.*) from $D_{\mathcal{X}\mathcal{Y}}$ with parameters θ . Then, the distribution of ID data is the marginal distribution of $D_{\mathcal{X}\mathcal{Y}}$ over \mathcal{X} , denoted as D_{in} . Conversely, the distribution of OOD data is represented as D_{out} , whose label set does not intersect with \mathcal{Y} . The primary objective of OOD detection is to determine whether a test input x originates from D_{in} or D_{out} . Typically, this decision is made using a score function S as follows:

$$G_\lambda(x) = \begin{cases} \text{ID} & \text{if } S(x, f) \geq \lambda, \\ \text{OOD} & \text{if } S(x, f) \leq \lambda, \end{cases}$$

where λ is a threshold. Samples with scores higher than λ are classified as ID data. The threshold is usually set based on ID data to ensure that a high fraction of ID data (e.g., 95%) is correctly identified as ID samples.

Finetune Model with Auxiliary OOD Data. In this paper, we consider the task of using auxiliary OOD data to fine-tune the model [14, 33, 35, 48], which can effectively enlarge the discrepancy between ID and unseen OOD data. Let's denote the auxiliary OOD dataset as D_{out}^{aux} , which is a subset of real OOD datasets but has different distributions from the test OOD datasets in the experiments for fair comparison. One classical method is the Outlier Exposure (OE, [14]), which designs an outlier exposure loss that calculates the cross-entropy function between OOD outputs and uniformly distributed labels. The equation is as follows:

$$L_{OE}(x) = -\frac{1}{C} \sum_{j=1}^C \log f_j(x) \quad (1)$$

where $f_j(x)$ denotes the j -th element of the model output $f(x)$. The final training objective of OE is to simultaneously minimize cross-entropy loss on ID data and

outlier exposure loss on OOD data, which can be formalized as:

$$\min_f \mathbb{E}_{(x,y) \sim D_{in}} L_{CE}(x, y) + \lambda \mathbb{E}_{x \sim D_{out}^{aux}} L_{OE}(x) \quad (2)$$

where λ is a hyper-parameter, usually set to 0.5. This optimization problem is regarded as a basic setting in auxiliary OOD data approaches. Most of subsequent methods adopt the same or similar loss functions that encourage ID and OOD data to differ in the output space. For example, POEM [35] designs a data sampling algorithm for efficient training, and DAL [48] employs adversarial features to calculate the OE loss to minimize the generalization gap between auxiliary and real unseen OOD data.

3.2 Motivation

Previous works have focused on increasing the discrepancy between ID and OOD data in the output space, while in this paper, we propose to explicitly enlarge the disparity of their features. Intuitively, separating features of ID and OOD data should be beneficial to OOD detection compared to solely augmenting the output differences. Existing feature separation functions in other fields, such as the dispersion loss that enlarges the distance between the average features of different classes [36, 20], are not suitable for diverse OOD data since their features are dispersed instead of clustering around the mean. To design a separation loss that can handle the complicated distribution of OOD features, we delve into the property of ID features. A recent observation named NC [40] gives us a new insight, which reveals that the penultimate features of ID samples within a class are nearly identical to the last layer weight of the corresponding class. This intriguing property has stimulated many fields of research, including low-dimensional characteristics of ID features [10, 41] and model generalization analysis [23, 16]. Particularly, several works employ the principal component spaces identified by NC to design score functions [32, 54, 12, 1], which demonstrates the large potential of NC applied in OOD detection. We conduct empirical experiments on CIFAR10 to validate the NC property, as Figure 2(a) shows. Furthermore, with the comparison of OOD features of vanilla and OE-trained model (Figure 2(a) *vs.* Figure 2(b)), we discover that although the outlier exposure loss only optimizes the output of OOD samples, it implicitly changes the distribution of OOD features, making OOD features more clustered and far way from ID features. However, from the 3D visualization of features in Figure 2(e), it can be observed that the features of OOD data almost lie in the same subspace as ID features, without taking advantage of the new dimension (z-axis) to further widen the ID-OOD difference. Based on the above observations, we then design a feature separation loss without modeling OOD feature distributions as follows.

3.3 Feature Separation Loss

Our key idea is to confine the features of OOD data to dimensions where ID features are sparsely distributed. Considering that the principal subspace of

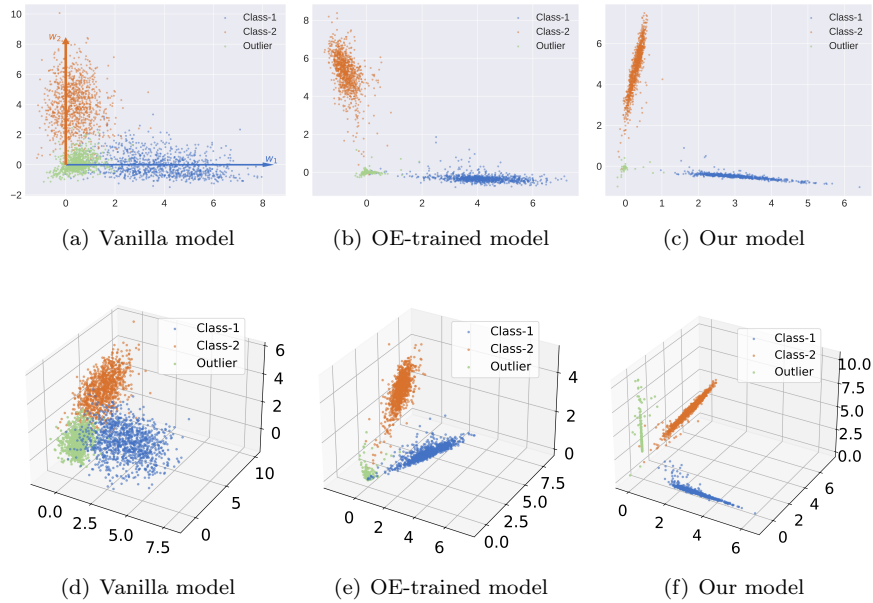


Figure 2: Visualization of features projected into the two-dimensional space consisted of w_1 and w_2 (ref. Figure 1) and the three-dimensional space consisted of w_1 , w_2 and the principal eigenvector of OOD features. The Class-1 and Class-2 represent features of ID samples of class-1 and class-2, and the Outlier means features of unseen OOD data. It can be observed that the feature separability between ID and OOD data gradually increases from left (Vanilla model) to right (Our model).

ID features is C -dimensional, as determined by the NC property, while the overall feature space has a significantly larger dimensionality, there exist ample redundant dimensions that can accommodate OOD features. In pursuit of our goal, a straightforward condition arises: $z^T w_i = 0, i = 1, 2, \dots, C$, where z denotes the normalized feature of OOD data, and w_i denotes the normalized fully connected layer weight for class i . According to this condition, we devise an OrthLoss for OOD data, which computes the average absolute value of the cosine similarity between z and w_i . The specific equation is as follows:

$$L_{Orth} = \frac{1}{C} \sum_{i=1}^C |z^T w_i| \quad (3)$$

Through minimizing the L_{Orth} loss, the OOD feature z tends to be distributed in the dimensions that are orthogonal to $w_i, i = 1, 2, \dots, C$. Figures 2(c) and 2(f) illustrate the features of our model fine-tuned using L_{Orth} . As observed, the features of outlier samples are indeed distributed in different dimensions from w_i , resulting in a larger discrepancy between ID and OOD features. Except for the L_{Orth} loss, we also propose an alignment loss that encourages ID features (denote as z_{ID}) within a class to align closely with the FC weight of their corresponding class (denote as w_y). We term this loss function as L_{NC} as it promotes neural collapse phenomenon [40], enabling ID features within a class more clustered. The formulation is as follows:

$$L_{NC} = -z_{ID}^T w_y \quad (4)$$

Our empirical experiment in Sec 4.3 indicates that adding L_{NC} in the training loss can further improve the detection performance. Combining the above two losses, the final optimization problem can be formulated as:

$$\min_f \mathbb{E}_{(x,y) \sim D_{in}} (L_{CE} + \alpha L_{NC}) + \mathbb{E}_{x \sim D_{out}^{aux}} (\lambda L_{OE} + \beta L_{Orth}) \quad (5)$$

where α and β are hyper-parameters, which are set to 1.0 in our experiments, λ maintains the common value in OE setting as 0.5.

3.4 Overall Framework

Training. Based on the optimization problem in Eq.5, we present the detailed training procedure as follows. Notably, the initial model for fine-tuning is not fully converged on the ID dataset, making the NC phenomenon less evident in the early training stages. Consequently, we propose a two-stage training process:

$$\begin{aligned} \text{Stage1: } & \min_f L_{CE} + \lambda L_{OE} \\ \text{Stage2: } & \min_f L_{CE} + \lambda L_{OE} + \alpha L_{NC} + \beta L_{Orth} \end{aligned} \quad (6)$$

In the first stage, we only utilize the cross-entropy and outlier exposure loss functions, similar to the OE method [14]. As long as the model tends to converge

on the ID dataset, we then incorporate L_{Orth} and L_{NC} into the training loss. In our experiments, we adopt a straightforward division where each stage occupies half of the total training epochs.

Test. After fine-tuning the model with our losses, we propose a new score function to detect OOD samples. Since our method simultaneously optimizes the output and feature of OOD data, a more proper score function is the sum of the traditional MSP [13] and the average cosine similarity between features and w_i . Mathematically, it can be expressed as:

$$S(x, f) = \max_i \frac{e^{y_i}}{\sum_j e^{y_j}} + \frac{1}{C} \sum_{i=1}^C |z^T w_i| \quad (7)$$

where y denotes the model output $f(x)$. Our experiments in Sec 4.4 compare the performance of using our score function with only using the MSP score. The result indicates that our method also performs well under MSP score, but slightly better under our proposed score function.

4 Experiments

In this section, we first conduct experiments on CIFAR10 and CIFAR100 benchmarks to validate the superiority of our method in Sec 4.1. Then, we consider the hard OOD detection setting proposed in [45] to further verify the effectiveness of our method in Sec 4.2. Subsequently, we evaluate our method under different settings in the ablation study section 4.3. In the last part, we discuss the fluctuation of performance, the influence of different score functions, and the numerical result of feature separation degree in Sec 4.4. To begin with, we introduce our experiment setups as follows. All the experiments are conducted on GPUs of NVIDIA GeForce RTX 4090.

OOD Datasets. We randomly choose 300K samples from the 80 Million Tiny Images [46] as our auxiliary OOD dataset. And we adopt five routinely used datasets as the test OOD datasets, including SVHN [38], LSUN [52], iSUN [51], Texture [7] and Places365[56], which have non-overlapping categories *w.r.t.* CIFAR datasets.

Pre-training Setups. We employ Wide ResNet-40-2 [53] trained for 200 epochs, with batch size 128, init learning rate 0.1, momentum 0.9, weight decay 0.0005, and cosine schedule.

Fine-tuning Setups. For both CIFAR10 and CIFAR100 benchmarks, we adopt the model parameter of the 99th epoch in the pre-training process as our initial network parameters, and then add auxiliary OOD data to train the model for 50 epochs with ID batch size 128, OOD batch size 256, initial learning rate 0.07, momentum 0.9, weight decay 0.0005 and cosine schedule. At the 25th epoch, we add our proposed L_{Orth} and L_{NC} into the training loss. The overall training setting is the same as DAL [48].

Compared Methods. We compare our method with post-hoc approaches, contrastive learning based methods, and auxiliary OOD data based methods. The

post-hoc methods include MSP[13], Energy[33], Maha[28], and KNN [44]. The contrastive learning based methods include CSI[45], CIDER[36], and KNN+[44]. The auxiliary OOD data based methods include OE [14], Energy-OE [33], POEM [35], and DAL [48]. For OE and Energy-OE, we adopt the same training setting as ours, since we have discovered that their recommended setting in the original paper performs much worse than our setting. For other methods, we adopt their suggested setups but unify the backbones for fairness.

Evaluation Metrics. We report two classical metrics in this paper: 1) FPR95: the false positive rate of OOD samples when the true positive rate of ID samples is at 95%. 2) AUROC: the area under the receiver operating characteristic curve. A lower FPR95 and a higher AUROC indicate better detection performance.

4.1 Main Results

The main results are shown in Table1, where we report the FPR95 and AUROC across the considered real OOD datasets ². Compared to methods based on vanilla or contrastive learning models, whose training datasets only contain ID samples, incorporating auxiliary OOD data into the training process can significantly reduce the FPR95 and improve the AUROC, indicating that this direction is valuable to explore. Compared to the classical OE approach [14], our method reduces the average FPR95 by 0.87% on CIFAR10 and 8.30% on CIFAR100, just by adding our OrthLoss and NcLoss in the second half stage of training procedures. This result demonstrates the effectiveness of our proposed feature separation loss. In addition to the OE approach, we also compare our method with other advanced works, including the classical work that studies data sampling strategies (POEM, [35]) and the adversarial feature augmentation work that aims to mitigate the impact of OOD distribution discrepancy (DAL, [48]). It is worth noticing that our method does not employ any data augmentation or selection algorithms, while we exhibit superior performances on CIFAR benchmarks. On CIFAR100, our method outperforms the best baseline DAL by 2.00% on FPR95 and 1.18% on AUROC. Based on the outstanding performance of our method, we suggest that our feature separation loss can be used as a basic training function like OE loss [14] considering its simplicity.

²The symbol * in the table means the results are cited from DAL [48]

Table 1: Results on CIFAR10 and CIFAR100 benchmarks. The best result is in bold.

Method	SVHN		LSUN		iSUN		Textures		Places365		Average	
	FPR95↓	AUROC↑	FPR95↓	AUROC↑	FPR95↓	AUROC↑	FPR95↓	AUROC↑	FPR95↓	AUROC↑	FPR95↓	AUROC↑
CIFAR-10												
With vanilla training												
MSP[13]	44.22	93.61	27.56	96.12	69.62	85.29	60.02	88.53	65.68	86.25	53.42	89.96
Energy[33]	31.81	94.65	4.6	98.96	50.06	89.75	49.68	90.09	42.28	90.82	35.69	92.854
Maha[28]	42.67	90.71	18.96	96.46	28.86	93.76	26.22	92.81	86.78	69.14	40.70	88.58
KNN[44]	44.76	92.55	27.38	95.34	43.84	91.24	37.64	92.82	49.23	87.89	40.57	91.97
With contrastive learning												
CSI*[45]	17.37	97.69	6.75	98.46	12.58	97.95	25.65	94.70	40.00	92.05	20.47	96.17
CIDER[36]	6.76	98.44	7.45	98.76	26.03	95.93	22.85	95.75	43.70	91.94	21.36	96.16
KNN+*[44]	3.28	99.33	2.24	98.90	17.85	97.65	10.87	97.92	30.63	94.98	12.97	97.32
With auxiliary OOD data												
OE[14]	1.40	99.54	0.85	99.64	2.20	99.26	2.80	99.26	9.55	97.39	3.36	99.02
Energy-OE[33]	0.75	99.50	0.90	98.98	1.50	99.22	2.75	98.92	9.05	97.33	2.99	98.79
POEM[35]	25.66	95.43	94.97	76.44	1.58	99.64	20.62	95.73	53.39	88.38	39.24	91.10
DAL[48]	0.75	99.28	0.75	99.62	0.70	99.33	2.35	98.99	8.90	97.10	2.69	98.86
Ours	0.40	99.28	0.60	99.68	1.60	99.25	2.45	98.83	7.40	97.60	2.49	98.93
CIFAR-100												
With vanilla training												
MSP[13]	74.79	79.64	54.72	86.46	93.85	56.92	88.76	68.48	83.24	71.95	79.07	72.69
Energy[33]	70.18	87.15	17.15	97.05	91.37	65.50	84.77	76.72	78.91	75.77	62.75	80.44
Maha[28]	77.73	78.01	98.46	63.44	47.74	88.76	54.93	82.53	97.22	54.11	75.22	73.37
KNN[44]	71.86	83.31	78.89	70.09	79.60	70.86	72.89	80.05	80.91	71.33	76.83	75.13
With contrastive learning												
CSI*[45]	64.50	84.62	25.88	95.93	70.62	80.83	61.50	86.74	83.08	77.11	61.12	95.05
CIDER[36]	16.47	96.23	45.45	81.64	66.01	82.21	49.79	87.48	82.66	68.39	52.08	83.19
KNN+*[44]	32.50	93.86	47.41	84.93	39.82	91.12	43.05	88.55	63.26	79.28	45.20	87.55
With auxiliary OOD data												
OE[14]	38.70	92.90	18.30	96.67	36.35	92.59	43.05	91.00	52.45	87.86	37.77	92.21
Energy-OE[33]	17.75	96.94	34.00	94.82	60.75	87.32	45.70	90.09	53.50	89.08	42.34	91.65
POEM[35]	45.41	90.70	3.01	99.24	18.60	95.79	51.37	83.85	84.13	73.93	40.5	88.87
DAL[48]	16.45	96.10	17.00	96.52	36.95	90.88	38.40	91.72	48.55	88.91	31.47	92.82
Ours	17.95	96.52	12.50	97.64	27.00	93.85	41.70	91.37	48.20	90.64	29.47	94.00

4.2 Hard OOD Detection

In addition to testing on the regular OOD datasets, we further consider three hard OOD datasets proposed in [45], which are considered more difficult to distinguish from ID samples. Following the same setting in [45, 44, 48], we evaluate our detection performance on LSUN-Fix [52], ImageNet-Resize [9] and CIFAR100 [24] with CIFAR10 as the ID dataset. Specific results are shown in Table 2. As we can see, our method shows comparable performance with DAL [48] over three hard OOD datasets, outperforming the baseline OE method by 2.55% on FPR95 on the ImageNet-Resize dataset.

4.3 Ablation Study

In this section, we conduct an ablation study to demonstrate the effectiveness of our proposed feature separation loss.

Choice of Training Loss.

Based on Eq.5, our objective loss function contains four parts: the first one is to ensure the accuracy on ID data,

Table 2: Hard OOD detection on CIFAR10 benchmark.

Methods	LSUN-Fix		ImageNet-Resize		CIFAR-100	
	FPR95↓	AUROC↑	FPR95↓	AUROC↑	FPR95↓	AUROC↑
With contrastive learning						
CSI*	39.79	93.63	37.47	93.93	45.64	87.64
CIDER	8.98	98.56	43.45	93.82	55.84	90.0
KNN+*	24.88	95.75	30.52	94.85	40.00	89.11
With auxiliary OOD data						
OE[14]	1.00	99.53	7.20	98.48	25.05	94.86
DAL[48]	0.65	99.59	3.75	98.63	26.00	94.35
Ours	0.75	99.07	4.65	98.42	24.60	94.69

and the rest three losses are to promote ID-OOD discrepancy.

To study their respective contribution to the detection performance, we adopt different settings of the training loss to fine-tune our model and report their corresponding average FPR95 and AUROC over five considered OOD datasets. The result is shown in Table 3. From it, we can discover that the addition of L_{Orth} can greatly improve the detection performance, and using L_{OE} , L_{NC} and L_{Orth} together achieves the best performance.

Table 3: Performance of our method under different training loss settings.

Method	L_{OE}	L_{NC}	L_{Orth}	CIFAR10		CIFAR100	
				FPR95↓	AUROC↑	FPR95↓	AUROC↑
OE [14]	✓	✗	✗	3.36	99.02	37.77	92.21
Ours-v1	✗	✓	✓	3.11	98.55	32.58	93.07
Ours-v2	✓	✓	✗	3.62	98.96	39.91	91.22
Ours-v3	✓	✗	✓	2.65	99.00	33.30	93.42
Ours	✓	✓	✓	2.49	98.93	29.47	94.00

Cosine Similarity vs. Euclidean Distance. Based on the NC property of ID features, an intuitive idea is to maximize the Euclidean distance between OOD features and weights of the last FC layer. In this part, we compare this Euclidean distance with our proposed OrthLoss which presents the cosine similarity actually. Since maximizing the Euclidean distance will cause its value to approach infinity, we instead use $\frac{1}{\|z-w_i\|}$ for OOD features and $\|z_{ID} - w_y\|$ for ID features as the training loss in the Euclidean distance setting, and then minimizing this loss to fine-tune the model. The comparison results are presented in Table 4, where the cosine similarity loss significantly outperforms Euclidean distance loss. The underlying reason may be that our OrthLoss utilizes new dimensions to separate ID and OOD features. When faced with unseen OOD data, the feature variations tend to fall on the new dimension, resulting in minimal changes in the output.

Table 4: Comparison between using the Euclidean distance and cosine similarity (ours) as the training loss to separate ID-OOD features.

Method	SVHN		LSUN		iSUN		Textures		Places365		Average	
	FPR95↓	AUROC↑	FPR95↓	AUROC↑	FPR95↓	AUROC↑	FPR95↓	AUROC↑	FPR95↓	AUROC↑	FPR95↓	AUROC↑
CIFAR-10												
Euclidean	1.70	99.48	1.15	99.60	3.20	99.22	4.55	98.95	12.55	95.97	4.63	98.64
Ours	0.40	99.28	0.60	99.68	1.60	99.25	2.45	98.83	7.40	97.60	2.49	98.93
CIFAR-100												
Euclidean	51.95	85.97	19.95	96.13	42.35	87.45	44.80	88.18	56.95	85.29	43.20	88.60
Ours	17.95	96.52	12.50	97.64	27.00	93.85	41.70	91.37	48.20	90.64	29.47	94.00

4.4 Discussion

Fluctuation in Detection Performance. We have observed considerable fluctuations in the performance of the DAL method [48] under repeated experiments with identical settings. Therefore, we evaluate the mean and variance of performance after repeating the same experiment five times. The results, shown

in Table 5, indicate that our approach exhibits greater stability, particularly on the CIFAR100 benchmark. Notably, even the OE method shows the FPR95 variance of 1.137 on CIFAR100, whereas our method maintains a variance of only 0.027.

Table 5: Fluctuation in detection performance of different methods.

Method	CIFAR10		CIFAR100	
	FPR95↓	AUROC↑	FPR95↓	AUROC↑
OE [14]	3.22 \pm 0.0017	99.07 \pm 0.0014	36.29 \pm 1.137	92.31 \pm 0.013
DAL [48]	2.87 \pm 0.0234	98.82 \pm 0.0027	30.44 \pm 2.216	93.07 \pm 0.075
Ours	2.49 \pm 0.0007	98.92 \pm 0.0033	29.50 \pm 0.027	93.98 \pm 0.014

Different Score Function. Since we use our proposed score function in Eq 7 to detect OOD samples while other auxiliary OOD data based methods only employ MSP score [13], in this part, we also evaluate our model with MSP score for a fair comparison. The results in Table 6 demonstrate that our approach also achieves commendable performance under the MSP score, with only a slight decline compared to using the proposed score function.

Table 6: Performance of adopting different score functions in our method.

Method	Score Function	CIFAR10		CIFAR100	
		FPR95↓	AUROC↑	FPR95↓	AUROC↑
Ours	MSP	2.77	98.76	29.96	93.27
	Eq. 7	2.49	98.93	29.47	94.00

Feature Separation Degree. In this part, we evaluate the degree of feature separation between ID and OOD data to validate the effectiveness of our proposed loss. Leveraging the NC property of ID features, we use the FC weight as the intermediary to design our measurement standards. Specifically, we propose three metrics, respectively defined by the Euclidean distance and cosine similarity between features and the weight of the predicted class, and the reconstruction error to the subspace spanned by FC weights. The results are shown in Table 7, where OOD means unseen test OOD data instead of auxiliary OOD samples. It can be seen that our model presents higher differences under the three metrics compared to vanilla and OE-trained models.

Table 7: Feature separation degree of different methods measured by three metrics. The higher difference (Diff) means better discrepancy between ID and OOD features.

Method	Euclidean Distance			Cosine Similarity			Reconstruction Error		
	ID	OOD	Diff↑	ID	OOD	Diff↑	ID	OOD	Diff↑
Vanilla	0.80	1.12	0.32	0.69	0.47	0.22	0.19	0.32	0.13
OE	0.86	1.21	0.35	0.79	0.32	0.47	0.41	0.83	0.42
Ours	0.69	1.16	0.47	0.75	$3e^{-5}$	0.75	0.43	0.86	0.43

5 Conclusion

In this paper, we propose a novel training loss designed to enhance the feature discrepancy between ID and OOD data during model fine-tuning with auxiliary OOD datasets. Given the inherent diversity and complexity of OOD sample distributions, we leverage the Neural Collapse property of ID features, which indicates that the penultimate features of ID samples within a class are nearly identical to the last layer weight of the corresponding class. Utilizing this property, we introduce a separation loss that confines OOD features to dimensions that are orthogonal to the principal subspace of ID features formed by NC. Our extensive experiments validate the effectiveness of our feature separation loss, achieving SOTA performance on CIFAR benchmarks. We believe that our study will inspire further research into pursuing feature discrepancy when employing auxiliary OOD data for model fine-tuning in OOD detection.

References

- [1] Mouïñ Ben Ammar, Nacim Belkhir, Sebastian Popescu, Antoine Manzanera, and Gianni Franchi. Neco: Neural collapse based out-of-distribution detection. *arXiv preprint arXiv:2310.06823*, 2023.
- [2] Haoyue Bai, Gregory Canal, Xuefeng Du, Jeongyeol Kwon, Robert D Nowak, and Yixuan Li. Feed two birds with one scone: Exploiting wild data for both out-of-distribution generalization and detection. In *International Conference on Machine Learning*, pages 1454–1471. PMLR, 2023.
- [3] T Cao, CW Huang, DYT Hui, and JP Cohen. A benchmark of medical out of distribution detection. arxiv 2020. *arXiv preprint arXiv:2007.04250*, 2007.
- [4] Dian Chen, Dequan Wang, Trevor Darrell, and Sayna Ebrahimi. Contrastive test-time adaptation. In *Proceedings of the IEEE/CVF Conference on Computer Vision and Pattern Recognition*, pages 295–305, 2022.
- [5] Jiefeng Chen, Yixuan Li, Xi Wu, Yingyu Liang, and Somesh Jha. Atom: Robustifying out-of-distribution detection using outlier mining. In *Machine Learning and Knowledge Discovery in Databases. Research Track: European Conference, ECML PKDD 2021, Bilbao, Spain, September 13–17, 2021, Proceedings, Part III 21*, pages 430–445. Springer, 2021.
- [6] Hyunsun Choi, Eric Jang, and Alexander A Alemi. Waic, but why? generative ensembles for robust anomaly detection. *arXiv preprint arXiv:1810.01392*, 2018.
- [7] Mircea Cimpoi, Subhransu Maji, Iasonas Kokkinos, Sammy Mohamed, and Andrea Vedaldi. Describing textures in the wild. In *Proceedings of the IEEE conference on computer vision and pattern recognition*, pages 3606–3613, 2014.

- [8] Matthew Cook, Alina Zare, and Paul Gader. Outlier detection through null space analysis of neural networks. *arXiv preprint arXiv:2007.01263*, 2020.
- [9] Jia Deng, Wei Dong, Richard Socher, Li-Jia Li, Kai Li, and Li Fei-Fei. Imagenet: A large-scale hierarchical image database. In *2009 IEEE conference on computer vision and pattern recognition*, pages 248–255. Ieee, 2009.
- [10] Connall Garrod and Jonathan P Keating. Unifying low dimensional observations in deep learning through the deep linear unconstrained feature model. *arXiv preprint arXiv:2404.06106*, 2024.
- [11] Jianping Gou, Baosheng Yu, Stephen J Maybank, and Dacheng Tao. Knowledge distillation: A survey. *International Journal of Computer Vision*, 129(6):1789–1819, 2021.
- [12] Jarrod Haas, William Yolland, and Bernhard Rabus. Linking neural collapse and l2 normalization with improved out-of-distribution detection in deep neural networks. *arXiv preprint arXiv:2209.08378*, 2022.
- [13] Dan Hendrycks and Kevin Gimpel. A baseline for detecting misclassified and out-of-distribution examples in neural networks. *arXiv preprint arXiv:1610.02136*, 2016.
- [14] Dan Hendrycks, Mantas Mazeika, and Thomas Dietterich. Deep anomaly detection with outlier exposure. *arXiv preprint arXiv:1812.04606*, 2018.
- [15] Rui Huang, Andrew Geng, and Yixuan Li. On the importance of gradients for detecting distributional shifts in the wild. *Advances in Neural Information Processing Systems*, 34:677–689, 2021.
- [16] Like Hui, Mikhail Belkin, and Preetum Nakkiran. Limitations of neural collapse for understanding generalization in deep learning. *arXiv preprint arXiv:2202.08384*, 2022.
- [17] Conor Igoe, Youngseog Chung, Ian Char, and Jeff Schneider. How useful are gradients for ood detection really? *arXiv preprint arXiv:2205.10439*, 2022.
- [18] Dihong Jiang, Sun Sun, and Yaoliang Yu. Revisiting flow generative models for out-of-distribution detection. In *International Conference on Learning Representations*, 2021.
- [19] Wenyu Jiang, Hao Cheng, Mingcai Chen, Chongjun Wang, and Hongxin Wei. Dos: Diverse outlier sampling for out-of-distribution detection. *arXiv preprint arXiv:2306.02031*, 2023.
- [20] Prannay Khosla, Piotr Teterwak, Chen Wang, Aaron Sarna, Yonglong Tian, Phillip Isola, Aaron Maschinot, Ce Liu, and Dilip Krishnan. Supervised contrastive learning. *Advances in neural information processing systems*, 33:18661–18673, 2020.

- [21] Durk P Kingma and Prafulla Dhariwal. Glow: Generative flow with invertible 1x1 convolutions. *Advances in neural information processing systems*, 31, 2018.
- [22] Ivan Kobyzev, Simon JD Prince, and Marcus A Brubaker. Normalizing flows: An introduction and review of current methods. *IEEE transactions on pattern analysis and machine intelligence*, 43(11):3964–3979, 2020.
- [23] Vignesh Kothapalli. Neural collapse: A review on modelling principles and generalization. *arXiv preprint arXiv:2206.04041*, 2022.
- [24] Alex Krizhevsky, Geoffrey Hinton, et al. Learning multiple layers of features from tiny images. 2009.
- [25] Solomon Kullback. *Information theory and statistics*. Courier Corporation, 1997.
- [26] Phuc H Le-Khac, Graham Healy, and Alan F Smeaton. Contrastive representation learning: A framework and review. *Ieee Access*, 8:193907–193934, 2020.
- [27] Jinsol Lee, Charlie Lehman, Mohit Prabhushankar, and Ghassan AlRegib. Probing the purview of neural networks via gradient analysis. *IEEE Access*, 11:32716–32732, 2023.
- [28] Kimin Lee, Kibok Lee, Honglak Lee, and Jinwoo Shin. A simple unified framework for detecting out-of-distribution samples and adversarial attacks. *Advances in neural information processing systems*, 31, 2018.
- [29] Jian Liang, Ran He, and Tieniu Tan. A comprehensive survey on test-time adaptation under distribution shifts. *arXiv preprint arXiv:2303.15361*, 2023.
- [30] Shiyu Liang, Yixuan Li, and Rayadurgam Srikant. Enhancing the reliability of out-of-distribution image detection in neural networks. *arXiv preprint arXiv:1706.02690*, 2017.
- [31] Jiashuo Liu, Zheyang Shen, Yue He, Xingxuan Zhang, Renzhe Xu, Han Yu, and Peng Cui. Towards out-of-distribution generalization: A survey. *arXiv preprint arXiv:2108.13624*, 2021.
- [32] Litian Liu and Yao Qin. Detecting out-of-distribution through the lens of neural collapse. *arXiv preprint arXiv:2311.01479*, 2023.
- [33] Weitang Liu, Xiaoyun Wang, John Owens, and Yixuan Li. Energy-based out-of-distribution detection. *Advances in neural information processing systems*, 33:21464–21475, 2020.
- [34] Julia Lust and Alexandru Paul Condurache. Gran: An efficient gradient-norm based detector for adversarial and misclassified examples. *arXiv preprint arXiv:2004.09179*, 2020.

- [35] Yifei Ming, Ying Fan, and Yixuan Li. Poem: Out-of-distribution detection with posterior sampling. In *International Conference on Machine Learning*, pages 15650–15665. PMLR, 2022.
- [36] Yifei Ming, Yiyu Sun, Ousmane Dia, and Yixuan Li. How to exploit hyperspherical embeddings for out-of-distribution detection? *arXiv preprint arXiv:2203.04450*, 2022.
- [37] Ibrahima Ndiour, Nilesh Ahuja, and Omesh Tickoo. Out-of-distribution detection with subspace techniques and probabilistic modeling of features. *arXiv preprint arXiv:2012.04250*, 2020.
- [38] Yuval Netzer, Tao Wang, Adam Coates, Alessandro Bissacco, Baolin Wu, Andrew Y Ng, et al. Reading digits in natural images with unsupervised feature learning. In *NIPS workshop on deep learning and unsupervised feature learning*, volume 2011, page 7. Granada, Spain, 2011.
- [39] Shuaicheng Niu, Jiaxiang Wu, Yifan Zhang, Yafo Chen, Shijian Zheng, Peilin Zhao, and Mingkui Tan. Efficient test-time model adaptation without forgetting. In *International conference on machine learning*, pages 16888–16905. PMLR, 2022.
- [40] Vardan Papyan, XY Han, and David L Donoho. Prevalence of neural collapse during the terminal phase of deep learning training. *Proceedings of the National Academy of Sciences*, 117(40):24652–24663, 2020.
- [41] Akshay Rangamani, Marius Lindegaard, Tomer Galanti, and Tomaso A Poggio. Feature learning in deep classifiers through intermediate neural collapse. In *International Conference on Machine Learning*, pages 28729–28745. PMLR, 2023.
- [42] Jingbo Sun, Li Yang, Jiaxin Zhang, Frank Liu, Mahantesh Halappanavar, Deliang Fan, and Yu Cao. Gradient-based novelty detection boosted by self-supervised binary classification. In *Proceedings of the AAAI Conference on Artificial Intelligence*, volume 36, pages 8370–8377, 2022.
- [43] Yiyu Sun, Chuan Guo, and Yixuan Li. React: Out-of-distribution detection with rectified activations. *Advances in Neural Information Processing Systems*, 34:144–157, 2021.
- [44] Yiyu Sun, Yifei Ming, Xiaojin Zhu, and Yixuan Li. Out-of-distribution detection with deep nearest neighbors. In *International Conference on Machine Learning*, pages 20827–20840. PMLR, 2022.
- [45] Jihoon Tack, Sangwoo Mo, Jongheon Jeong, and Jinwoo Shin. Csi: Novelty detection via contrastive learning on distributionally shifted instances. *Advances in neural information processing systems*, 33:11839–11852, 2020.

- [46] Antonio Torralba, Rob Fergus, and William T Freeman. 80 million tiny images: A large data set for nonparametric object and scene recognition. *IEEE transactions on pattern analysis and machine intelligence*, 30(11):1958–1970, 2008.
- [47] Haoqi Wang, Zhizhong Li, Litong Feng, and Wayne Zhang. Vim: Out-of-distribution with virtual-logit matching. In *Proceedings of the IEEE/CVF conference on computer vision and pattern recognition*, pages 4921–4930, 2022.
- [48] Qizhou Wang, Zhen Fang, Yonggang Zhang, Feng Liu, Yixuan Li, and Bo Han. Learning to augment distributions for out-of-distribution detection. *Advances in Neural Information Processing Systems*, 36, 2024.
- [49] Qizhou Wang, Junjie Ye, Feng Liu, Quanyu Dai, Marcus Kalander, Tongliang Liu, Jianye Hao, and Bo Han. Out-of-distribution detection with implicit outlier transformation. *arXiv preprint arXiv:2303.05033*, 2023.
- [50] Yingwen Wu, Tao Li, Xinwen Cheng, Jie Yang, and Xiaolin Huang. Low-dimensional gradient helps out-of-distribution detection. *arXiv preprint arXiv:2310.17163*, 2023.
- [51] Pingmei Xu, Krista A Ehinger, Yinda Zhang, Adam Finkelstein, Sanjeev R Kulkarni, and Jianxiong Xiao. Turkergaze: Crowdsourcing saliency with webcam based eye tracking. *arXiv preprint arXiv:1504.06755*, 2015.
- [52] Fisher Yu, Ari Seff, Yinda Zhang, Shuran Song, Thomas Funkhouser, and Jianxiong Xiao. Lsun: Construction of a large-scale image dataset using deep learning with humans in the loop. *arXiv preprint arXiv:1506.03365*, 2015.
- [53] Sergey Zagoruyko and Nikos Komodakis. Wide residual networks. *arXiv preprint arXiv:1605.07146*, 2016.
- [54] Jiawei Zhang, Yufan Chen, Cheng Jin, Lei Zhu, and Yuantao Gu. Epa: Neural collapse inspired robust out-of-distribution detector. *arXiv preprint arXiv:2401.01710*, 2024.
- [55] Haotian Zheng, Qizhou Wang, Zhen Fang, Xiaobo Xia, Feng Liu, Tongliang Liu, and Bo Han. Out-of-distribution detection learning with unreliable out-of-distribution sources. *Advances in Neural Information Processing Systems*, 36, 2024.
- [56] Bolei Zhou, Agata Lapedriza, Aditya Khosla, Aude Oliva, and Antonio Torralba. Places: A 10 million image database for scene recognition. *IEEE transactions on pattern analysis and machine intelligence*, 40(6):1452–1464, 2017.

- [57] Yao Zhu, YueFeng Chen, Chuanlong Xie, Xiaodan Li, Rong Zhang, Hui Xue, Xiang Tian, Yaowu Chen, et al. Boosting out-of-distribution detection with typical features. *arXiv preprint arXiv:2210.04200*, 2022.
- [58] Ev Zisselman and Aviv Tamar. Deep residual flow for out of distribution detection. In *Proceedings of the IEEE/CVF Conference on Computer Vision and Pattern Recognition*, pages 13994–14003, 2020.

A Appendix / supplemental material

A.1 Limitations

Our approach requires an auxiliary OOD dataset and a fine-tuning process. But for real-world applications, it is more practical to detect directly based on a pre-trained model. This is a general limitation for auxiliary OOD data based approaches. A possible solution is to use auxiliary OOD data during the test phase by designing test-time adaptation algorithms [29, 4, 39], thereby obviating the training process but maintaining outstanding detection performance.